Certifiably Optimal Doppler Positioning using Opportunistic LEO Satellites

BAOSHAN SONG
The Hong Kong Polytechnic University, Hong Kong SAR, China

WEISONG WEN, Member, IEEE
The Hong Kong Polytechnic University, Hong Kong SAR, China

QI ZHANG
The Hong Kong Polytechnic University, Hong Kong SAR, China

BING XU, Member, IEEE
The Hong Kong Polytechnic University, Hong Kong SAR, China

LI-TA HSU, Senior Member, IEEE
The Hong Kong Polytechnic University, Hong Kong SAR, China

Abstract— **To provide backup and augmentation to global navigation satellite system (GNSS), Doppler shift from Low Earth Orbit (LEO) satellites can be employed as signals of opportunity (SOP) for position, navigation and timing (PNT). Since the Doppler positioning problem is non-convex, local searching methods may produce two types of estimates: a global optimum without notice or a local optimum given an inexact initial estimate. As exact initialization is unavailable in some unknown environments, a guaranteed global optimization method in no need of initialization becomes necessary. To achieve this goal, we propose a certifiably optimal LEO Doppler positioning method by utilizing convex optimization. In this paper, the certifiable positioning method is implemented through a graduated weight approximation (GWA) algorithm and semidefinite programming (SDP) relaxation. To guarantee the optimality, we derive the necessary conditions for optimality in ideal noiseless cases and sufficient noise bounds conditions in noisy cases. Simulation and real tests are conducted to evaluate the effectiveness and robustness of the proposed method. Specially, the real test using Iridium-NEXT satellites shows that the proposed method estimates an certifiably optimal solution with an**

Authors' addresses: Baoshan Song is with The Hong Kong Polytechnic University, Hong Kong, SAR, China, E-mail: (baoshan.song@connect.polyu.hk); Weisong Wen is with The Hong Kong Polytechnic University, Hong Kong, SAR, China, E-mail: (welson.wen@polyu.edu.hk); Qi Zhang is with The Hong Kong Polytechnic University, Hong Kong, SAR, China, E-mail: (qi915.zhang@connect.polyu.hk); Bing Xu is with The Hong Kong Polytechnic University, Hong Kong, SAR, China, E-mail: (pbing.xu@polyu.edu.hk); Li-Ta Hsu is with The Hong Kong Polytechnic University, Hong Kong, SAR, China, E-mail: (lt.hsu@polyu.edu.hk). (Corresponding authors: Li-Ta Hsu)

The open-source code and data are open-sourced at https://github.com/Baoshan-Song/Certifiable-Doppler-positioning.

Color versions of one or more of the figures in this article are available online at http://ieeexplore.ieee.org.

3D positioning error of 140 m without initial estimates while Gauss-Newton and Dog-Leg are trapped in local optima when the initial point is equal or larger than 1000 km away from the ground truth. Moreover, the certifiable estimation can also be used as initialization in local searching methods to lower down the 3D positioning error to 130 m.

Index Terms— **LEO satellite, Doppler positioning, signal of opportunity, convex optimization, semidefinite programming.**

I. INTRODUCTION

LEO satellite is an alternative and a supplement to GNSS in providing PNT services. Position, navigation and timing (PNT) services have great importance in the modern society [1]. In the past decades, GNSS is considered as the leading approach to providing PNT services. However, there are many challenges for traditional GNSS, such as signal blocking [2], jamming [3] and spoofing [4]. Failure of GNSS could lead to large-scale disruption and financial loss up to huge amount of dollars [5]. In recent years, LEO satellite has been employed as an alternative and a supplement to GNSS, since LEO satellites have advantages in signal strength, rapid geometry changes, and abundant sources [6]. By the end of 2023, there are about 8400 LEO satellite in the space, which are of great potential for PNT services. These satellites can be mainly divided into two categories: (1) One is the navigation satellite with designed payloads and signals. For example, Xona has announced a new constellation named PULSAR for PNT services [7]. In general, the number of satellites from dedicated navigation constellations is relatively small. (2) The other is the non-navigation satellite designed for other purposes such as communication and scientific research. At present, most of the LEO constellations in operation, including OneWeb, Orbcomm and Starlink etc., are not designed specifically for navigation. This means that unauthorized users are not allowed to receive navigation information from these satellites, such as pseudorange and broadcast ephemeris [8]. Luckily, there is still possibility to use the non-navigation LEO satellites for PNT services, such as signals of opportunity (SOP) [9]. Considering the potential of LEO mega-constellations, in this paper, we focus on using a direct product–Doppler shift that derived from the LEO SOP for positioning.

Doppler positioning with LEO satellite is ready but requires exact initial estimation. Among LEO SOP measurements, the Doppler shift measurement of the carrier signal is widely used, as it is a primary product in signal acquisition and tracking [10]. As a classic method, the concept of LEO Doppler positioning is not new and the first system is Transit [11] which started to provide a continuous navigation service from 1964. After decades, the past few years have heralded a new era in LEO [12] with the construction of mega-LEO constellations. To utilize opportunistic signals from all these satellites, researchers have found three types of unknown parameters in LEO opportunistic navigation [13]: (1) downlink signal structure, (2) satellite clock error and (3)
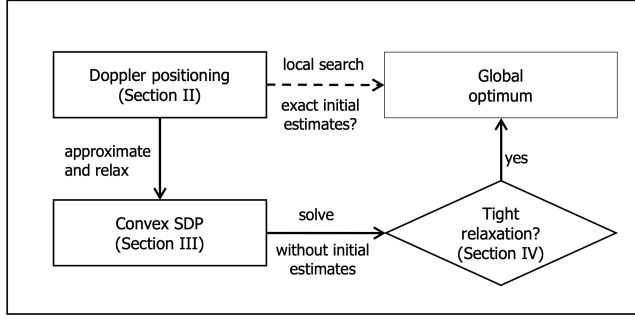
Fig. 1. Certifiably optimal LEO Doppler positioning framework. Compared . Two contributions are proposed: convex SDP in Section III and tight relaxation conditions in Section IV.

ephemeris. These parameters are easily accessible from GNSS but difficult for non-cooperative LEO satellites. In the recent literature, some solutions are available to ease these burdens, such as [14], [15]. However, there is still one critical problem: most of current LEO Doppler positioning methods employ local optimization which relies on exact initial estimation guess. For example, [16] has proved that the initial receiver position with error less than 300 km is necessary if the satellites is at the orbit at the height of 550 km. This is because the mathematical model of LEO Doppler positioning is nonlinear and thus containing multiple locally optimal points. Therefore, using local optimization in LEO Doppler positioning is possibly dangerous when it is difficult to obtain an exact initial position. To optimize the LEO Doppler problem to a globally optimal solution without precise initialization, it is necessary to employ knowledge from other domains.

Convex optimization without initial estimation opens a new window. Thanks to the development of computing platform and optimization theory, it is possible to generate a globally optimal solution for some questions. According to [17], what matters to a unique global optima is not nonlinearity but non-convexity. With Lagrangian duality, it is possible to relax an original non-convex problem to a convex problem. By solving the convex dual problem, we can obtain the lower bound of the objective function value in the non-convex problem. The difference between original-relaxed objective function values is defined as duality gap. Under certain conditions, it is possible that duality gap is zero and we can recover the globally optimal solution of the original non-convex problem. This kind of method has been utilized in many robotic works, including geometric registration [18], sensor calibration [19], simultaneous localization and mapping (SLAM) [20], rotation synchronization [21], camera arrangements [22], indoor positioning [23] and wireless localization [24]. However, there is still a gap at the application of convex optimization on the LEO Doppler positioning problem.

To fill this gap, this paper aims to construct a certifiably optimal LEO Doppler positioning system and open-source the proposed software and related data. This work builds on our earlier development of a certifiably optimal Doppler-based orbit determination (OD) method for LEO satellites [25], extending the convex optimization framework to the positioning of ground receivers using opportunistic LEO Doppler measurements. While the prior work focused on estimating satellite orbits from ground-based observations, this manuscript addresses the more challenging and underexplored inverse problem: determining ground user positions from non-cooperative satellite Doppler data without requiring initial guesses.

To the best of our knowledge, this is the first certifiably optimal LEO Doppler positioning system in no need of initial estimation. The main contributions of this article are as follows:

- **Model LEO Doppler positioning using convex relaxation:** We propose a novel LEO Doppler positioning framework, using semidefinite relaxation to transform original Doppler positioning problem (non-convex) to a semidefinite programming (SDP) problem (convex). Then we can solve the SDP problem using off-the-shelf solvers and recover the solution of original Doppler positioning problem.
- **Analyze relaxation tightness and robustness:** The duality gap between the objective costs from the original and relaxed problem determines the solution's optimality. Therefore, together with the relaxation framework, we analyze the conditions for zero-duality gap in both noiseless and noisy cases, which certifies a unique solution under parameter disturbances.
- **Experimental verification:** Both simulation and real tests are conducted to evaluate the performance of the proposed system compared with local estimation based methods. To contribute to the community, we also open source all the codes and data we have mentioned.

The remainder of this paper is organized as follows. Section II introduces the general Doppler positioning model and reveals the challenges. Section III derives the proposed certifiable positioning method using approximation and semidefinite relaxation. After that, Section IV presents the performance guarantee analysis using Lagrangian duality and constraint qualification. Then Section V evaluate the performance of proposed system by simulation and real-world experiments. Finally, Section VI discusses about conclusions and future works.

Notation: lowercase and uppercase denote vector and matrix, both of which are written in boldface (e.g. $\mathbf{a}$ and $\mathbf{A}$). $\text{diag}\{a_1,...,a_n\}$ denotes a diagonal matrix with elements $a_1,...,a_n$. $\mathbf{a}_{(i:j)}$ denotes the i-th to j-th components of $\mathbf{a}$ and $\mathbf{A}_{(i:j)}$ is the submatrix of $\mathbf{A}$ with corners $(i,i),(i,j),(j,i),(j,j)$. $\mathbf{I}_n$ denotes a $n \times n$ identity matrix. $\text{rank}(\mathbf{A})$ and $\text{tr}(\mathbf{A})$ denote the rank and trace of square matrix $\mathbf{A}$ separately. $\mathbb{R}^n$ and $\mathbb{S}^n$ denote n dimension real space and $n \times n$ symmetric matrix space. $\mathbf{A} \succeq 0$ means $\mathbf{A}$ is positive semidefinite. 2-norm of a matrix $\mathbf{A}$ or a
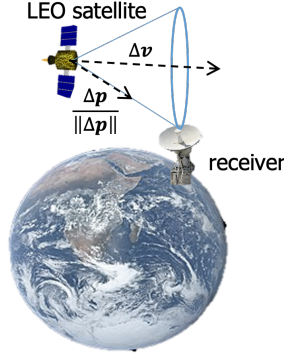
Fig. 2.   LEO Doppler positioning illustration.

vector $\mathbf{a}$ is $\|\mathbf{A}\|$ or $\|\mathbf{a}\|$. $\mathbf{A} \bullet \mathbf{B}$ denotes the Frobenius inner product of the two matrices.

II.   LEO Doppler positioning problem

This paper focuses on the static LEO Doppler positioning problem (simplified as Doppler positioning problem in the follows) and provides a basic paradigm for Doppler positioning. In this kind of problem, we are given the Doppler shift measurement such as D output by a LEO SOP receiver. There are various types of errors included in the LEO Doppler measurement, such as satellite-related, transmission-related and receiver-related errors. According to [16], most of the errors could be corrected or ignored. After the correction of main systematic errors, the LEO Doppler shift measuring model between a satellite s and a receiver r can be modeled as:

$$D = (\mathbf{p}_r - \mathbf{p}^s)^T (\mathbf{v_r} - \mathbf{v}^s)/\rho + c \cdot d\dot{t}_r + \varepsilon \qquad (1)$$

where D is the Doppler shift measurement (m/s); $\mathbf{p}_r$ and $\mathbf{p}^s$ are the position of the receiver and the satellite (m); ρ is the geometric distance between the phase center of the satellite and receiver $(\rho = \|\mathbf{p}_r - \mathbf{p}^s\|)$ (m); $\mathbf{v_r}$ and $\mathbf{v}^s$ are the velocity of the receiver and the satellite (m/s); c is the speed of light (m/s); $d\dot{t}_r$ is the clock shift rate of the receiver (Hz); ε is the additive Gaussian white noise (m/s). Given the Doppler measuring model (1), we also illustrate the Doppler shift measuring model in Fig. 2. This related geometric model is adopted in [10][16]. As the figure shows, the Doppler shift measurement can be considered as a projection of relative velocity between a ground receiver and a satellite in the direction of the line-of-sight (LOS) vector, with all Doppler shifts forming a conical surface with the satellite as the vertex. Therefore, if there are abundant Doppler shifts, the receiver will be located at the intersection of the conical surfaces. Since there could be many intersection points, the Doppler positioning problem includes multiple locally feasible solutions.

Given N Doppler shift measurements $[D_1, ..., D_N]^T$, the static Doppler positioning problem could be modeled

as a nonlinear weighted least squares (NWLS) problem:

$$\min_{\mathbf{p}_r, d\dot{t}_r} \sum_{i=1}^{N} \left\| D_i - (\mathbf{p}_r - \mathbf{p}^s)^T \mathbf{v}^s / \rho_i - c \cdot d\dot{t}_r \right\|_{\mathbf{Q}_\varepsilon} \qquad (2)$$

where

$$\mathbf{Q}_\varepsilon = I_N \cdot \varepsilon_D \qquad (3)$$

However, searching the global optima of a general NWLS problem is difficult [26]. In the other words, there is no closed-form solution and we have to employ numerical optimization methods to solve it. From the previous view of nonlinearity, the problem is nonlinear due to the square function and the nonlinear residual function. In most previous studies, a nonlinear problem is usually solved with linear approximation using local searching methods such as Gauss-Newton [27]. Unfortunately, these methods rely on exact initial estimates and cannot provide optimality guarantees. In this paper, we dispose the non-convex property of the NWLS problem and use convex relaxation to solve it. To fill this gap, we revealing its nonconvexity rather than nonlinearity, thus pointing out the main challenges and possibilities of our certifiable method in the next section. According to [17], there are three kinds of nonconvex functions here: *(i) fractional; (ii) polynomial and (iii) square functions*. The main challenge is to relax these nonconvex functions to convex ones. Although the problem (2) is NP-hard, we show how to perform convex relaxation and solve the new problem using convex optimization methods in the next section.

III.   Certifiable Doppler positioning

In general, a local searching method is easy to formulate but difficult to solve globally, while a convex relaxation method is complex to formulate but easy to solve globally [17]. In this section, we propose a certifiable approach to solve LEO Doppler positioning based on approximation and convex relaxation. This section will derive the approach which works as follows:

- Fractional part : we approximate the NWLS problem (2) as a polynomial optimization problem (POP) (4) in Section A;
- Polynomial part: we lift the POP (4) to a quadratically constrained quadratic program (QCQP) (7) in Section B;
- Square part: we relax the QCQP (7) to a semidefinite program (SDP) (11) in Section C.

We describe each step as follows.

A.   POP formulation

As a first step, this section disposes the nonconvex fractional part of the cost function by a POP approximation. A POP is an optimization problem where both the objective function and all constraints are multivariate polynomials. According to Lasserre's global optimization hierarchy, it is possible to solve the global optima of a

polynomial optimization problem. Therefore, we reformulate (2) by multiplying the cost function with the range ρ_i, after which we get a problem with changeable weighting:

$$\min_{\mathbf{p}_r, \dot{di}} \sum_{i=1}^{N} \left\| \rho_i \cdot D_i + (\mathbf{p}_r - \mathbf{p}_i^s)^T \mathbf{v}_i^s - c \cdot \rho_i \cdot \dot{di}_r \right\|_{\mathbf{Q}}^2 \tag{4}$$

where $\mathbf{Q}$ is related to variable $[\rho_1, ..., \rho_N]^T$:

$$\mathbf{Q} = \mathrm{diag}\{1/\rho_1, ..., 1/\rho_N\} * \varepsilon_D \tag{5}$$

After this reformulation, there is still one problem: $\mathbf{Q}$ is not constant and linear to the satellite-receiver geometric range ρ. To fill this gap, we propose a *graduated weighting approximation* algorithm and the detail is shown in Algorithm 1. The key insight here is that in LEO satellite positioning cases, we find that all the range $[\rho_1, ..., \rho_N]^T$ are closed, so it is acceptable to use ε_D to approximate ε_D/ρ in the first estimation. Afterwards we can substitute latest estimate of ρ to recalculate the noise ε_D/ρ for more accurate estimation. In the other words, in each iteration in Algorithm 1, the problem (4) is estimated with a constant weighting and thus can be treated as a POP in the following sections. Similar ideas have also been used in previous works [28].

Algorithm 1 Graduated Weighting Approximation

Require: maximum number of iteration T (default T=1000); initial $\mathbf{Q}$ (default $\mathbf{Q}^{(0)} = I$); initial η (default $\eta = +\infty$); initial $\bar{\eta}$ (deault $\bar{\eta} = 0.1\%$).
1: % approximate the true weighting by iteration
2: **for** $t = 0, ..., T$ **do**
3:    % construct coefficient matrix
4:    $\mathbf{F}^{(t)} = \mathbf{A}^T {\mathbf{Q}^{(t)}}^{-1} \mathbf{A}, \mathbf{l}_0^{(t)} = 2\mathbf{k}^T {\mathbf{Q}^{(t)}}^{-1} \mathbf{A}$
5:    % get ρ by solving the SDP problem (11)
6:    $[\rho_1^{(t)}, ..., \rho_N^{(t)}]^T = \mathrm{solve\_SDP}(\mathbf{F}^{(t)}, \mathbf{l}_0^{(t)})$
7:    % compute new weighting matrix using (5)
8:    $\mathbf{Q}^{(t)} = \mathrm{diag}\{1/\rho_1^{(t)}, ..., 1/\rho_N^{(t)}\} * \varepsilon_D$
9:    **if** $t > 0$ **then**
10:      $\eta^{(t)} = \mathrm{tr}(\mathbf{Q}^{(t)} - \mathbf{Q}^{(t-1)})$
11:    **end if**
12:    **if** $\eta^{(t)} < \bar{\eta}$ **then**
13:      break
14:    **end if**
15: **end for**
16: **return** $\mathbf{Q}^{(t)}$

B. QCQP formulation

Although some existing methods can directly solve a POP, they may be computationally expensive [29]. To solve the POP in polynomial time, we have to reformulate the polynomial residual function to a linear function with constraints. As a result, the composite function of the linear residual and least square functions is written as a QCQP. According to [30], a QCQP could be efficiently solved to a global optimum by SDP methods in polynomial time. To reformulate a POP to a QCQP, the first step is *lifting variables* [31]. Lifting variables in [31] means

introducing higher dimensional variables (e.g., matrices) to transform nonlinear terms into linear ones, enabling convex relaxation of a non-convex problem. We follow this method to transform state variable and we get a lifted state vector:

$$\mathbf{y} = [\mathbf{p}_r^T, c \cdot \dot{di}_r, \rho_1, ..., \rho_N, z_1, ..., z_N]^T \tag{6}$$

where $z_i = c \cdot \rho_i \cdot \dot{di}_r, \ i = 1, ..., N$. Compared to the state in the POP (4), the lifted state vector introduces more variables that are related to the monomials in the squares. After lifting variables, the second step of reformulation is *adding constraints*. This is because there is information loss during the lifting. To obtain a lossless lifted problem, we also need to employ redundant constraints to describe the connection inside the lifted state vector. In this paper, the connection between lifted variables are obvious and the constraints are derived directly. After adding redundant constraints, the POP (4) can be written as a QCQP:

$$
\begin{aligned}
\min_{\mathbf{y}} \ & \mathrm{tr}(\mathbf{A}^T \mathbf{Q}^{-1} \mathbf{A} \mathbf{Y}) + 2\mathbf{k}^T \mathbf{Q}^{-1} \mathbf{A} \mathbf{y} + \mathbf{k}^T \mathbf{k} \\
\text{s. t. } & y_{(4+i)}^2 = \mathrm{tr}(\mathbf{Y}_{(1:3)}) - 2\mathbf{p}^{s_i T} \mathbf{y}_{(1:3)} + \mathbf{p}^{s_i T} \mathbf{p}^{s_i}, \\
& \mathbf{y}_{(4+N+i)} = \mathbf{Y}_{(4,4+i)} \\
& \mathbf{Y} = \mathbf{y}\mathbf{y}^T, \quad i = 1, ..., N
\end{aligned} \tag{7}
$$

where

$$\mathbf{A} = \begin{bmatrix} \mathbf{v}^{s_1 T} & 0 & D_1 & ... & 0 & -1 & ... & 0 \\ \vdots & \vdots & \vdots & \ddots & \vdots & \vdots & \ddots & \vdots \\ \mathbf{v}^{s_N T} & 0 & 0 & ... & D_N & 0 & ... & -1 \end{bmatrix} \tag{8}$$

$$\mathbf{k} = \begin{bmatrix} -\mathbf{p}^{s_1 T} \mathbf{v}^{s_1} & ... & -\mathbf{p}^{s_N T} \mathbf{v}^{s_N} \end{bmatrix}^T \tag{9}$$

C. Semidefinite relaxation

In this section, we dispose the square function part and derive SDP relaxation on QCQP (7) to get a convex problem. It has been proven that a QCQP problem (7) is still nonconvex, so we apply Shor's relaxation to relax the relationship between the vector $\mathbf{y}$ and the symmetric matrix $\mathbf{Y}$. According to QCQP (7), the only one nonconvex constraint is $\mathbf{Y} = \mathbf{y}\mathbf{y}^T$ and it is equivalent to

$$
\begin{aligned}
\begin{bmatrix} \mathbf{Y} & \mathbf{y} \\ \mathbf{y}^T & 1 \end{bmatrix} &\succeq 0 \\
\mathrm{rank}(\mathbf{Y}) &= 1
\end{aligned} \tag{10}
$$

In short, Shor's relaxation means ignoring the rank-1 constraint and derive a SDP problem from the QCQP (7):

$$
\begin{aligned}
\min_{\mathbf{S} \in \mathbb{S}^{2N+5}} \ & \mathbf{F} \bullet \mathbf{Y} + \mathbf{l}_0 \mathbf{y} + c_0 \\
\text{s. t. } & \mathbf{S} = \begin{bmatrix} \mathbf{Y} & \mathbf{y} \\ \mathbf{y}^T & 1 \end{bmatrix} \succeq 0 \\
& \mathbf{G_i} \bullet \mathbf{Y} + \mathbf{l_i}\mathbf{y} + c_i = 0 \qquad i = 1, ..., 2N
\end{aligned} \tag{11}
$$

where

$$\mathbf{F} = \mathbf{A}^T\mathbf{Q}^{-1}\mathbf{A}$$
$$\mathbf{l}_0 = 2\mathbf{k}^T\mathbf{Q}^{-1}\mathbf{A}$$
$$c_0 = \mathbf{k}^T\mathbf{k}$$
$$\mathbf{G}_i = \mathrm{diag}\{[\mathbf{1}_3^T, 0, -\mathbf{e}_i^T, \mathbf{0}_{1\times N}]^T\}$$
$$\mathbf{l}_i = \begin{bmatrix} -2\mathbf{p^{s_i}}^T & \mathbf{0}_{1\times(2N+1)} \end{bmatrix}$$
$$c_i = \mathbf{p^{s_i}}^T\mathbf{p^{s_i}}$$
$$\mathbf{G}_{i+N} = \begin{bmatrix} \mathbf{0}_{3\times3} & \mathbf{0} & \mathbf{0} \\ \mathbf{0} & \mathbf{E}_i & \mathbf{0} \\ \mathbf{0} & \mathbf{0} & \mathbf{0}_{N\times N} \end{bmatrix} \qquad (12)$$
$$\mathbf{E}_i = \begin{bmatrix} 0 & \frac{1}{2}\mathbf{e}_i^T \\ \frac{1}{2}\mathbf{e}_i & \mathbf{0}_{N\times N} \end{bmatrix}_{(1+N)\times(1+N)}$$
$$\mathbf{l}_{i+N} = \begin{bmatrix} \mathbf{0}_{1\times4} & \mathbf{e}_i^T & 0 \end{bmatrix}$$
$$c_{i+N} = 0$$
$$i = 1, ..., N$$

where $\mathrm{diag}\{\mathbf{a}\}$ denotes a diagonal matrix with the elements of vector $\mathbf{a}$ on its main diagonal and zeros elsewhere, $\mathbf{0}_{m\times n}$ is a $m \times n$ all-zero matrix, $\mathbf{1}_n$ is a n-dimensional all-one vector, and $\mathbf{e}_i$ is a N-dimensional standard basis vector with a 1 at the i-th position and 0 elsewhere.

In fact, this transformation is one of the key concept in this paper: we formulate an SDP relaxed problem (convex with a unique solution) instead of a rank-constrained QCQP problem (non-convex with multiple solutions). In the following, we will solve the SDP relaxed problem by Lagrangian duality and resume the unique solution of the QCQP problem by rank-1 conditions.

In summary, three steps in this Section III transform a nonconvex NWLS problem into a convex SDP. Now we can employ off-the-shelf SDP solvers to globally solve the SDP. In the next section, we will recover the optimal estimation of the NWLS prolem from the SDP in certain conditions and discuss the performance with both noiseless and noisy measurements.

IV. Performance Guarantees

In previous sections, we derive a SDP whose cost is the lower bound of original NWLS problem cost. We have already prove the GWA and lifting variables are lossless. Therefore, to achieve zero gap between SDP-NWL costs, we have to obatin *tight relaxation* in the SDP relaxation (in Section C) so that we can resume the unique NWLS optimum from the SDP solution. In this section, we discuss the conditions for tight relaxation by the Lagrangian duality theorem.

A. Lagrangian Duality

To give necessary conditions of tight SDP relaxation, we follow the homogeneous formulation in [31] and apply Lagrangian duality to the SDP (11) and its dual problem

of can be written as:

$$\max_\lambda \mathbf{0}$$
$$\text{s. t. } \mathbf{H}(\lambda) \succeq 0,$$
$$\mathbf{H}(\lambda) = \begin{bmatrix} \mathbf{c_0} & \mathbf{l_0}^T \\ \mathbf{l_0} & \mathbf{F} \end{bmatrix} + \sum_{i=1}^{2N} \lambda_i \begin{bmatrix} \mathbf{c_i} & \mathbf{l_i}^T \\ \mathbf{l_i} & \mathbf{G_i} \end{bmatrix} \qquad (13)$$

where $\lambda \in \mathbb{R}^m$ is the Lagrangian multiplier vector of equation constraints.

B. Tightness in a noiseless case

We use q^*, p^* and d^* to denote the optimal cost of QCQP (7), SDP primal (11) and SDP dual (13) problems. The relationship between them is $q^* \geq p^* \geq d^*$. In fact, if we can provide $q^* = p^* = d^*$ and $\mathrm{rank}(\mathbf{Y}) = 1$, i.e. *rank-tightness* in [31], we can resolve the globally optimal OD solutions. To achieve this goal, we will discuss about the necessary conditions for certifiably correct estimation in both noiseless and noise cases in the follows. To simplify the notations, we use $f(\mathbf{y})$ and $g_i(\mathbf{y}), i = 1, ..., 2N$ to denote the cost function and constraint functions. By applying the Karush–Kuhn–Tucker (KKT) conditions [30], we can find the sufficient conditions of zero duality gap between primal problem (11) and dual problem (13):

(i) $g_i(\mathbf{y}) = 0, \quad i = 1, ..., N$
(ii) $\mathbf{H}(\lambda) \succeq 0$
(iii) $\mathbf{H}(\lambda)[1, \mathbf{y}^T]^T = 0$

According to [31], $\mathrm{rank}(\mathbf{Y}) = 1$ is the sufficient-and-necessary condition for tightness in Shor's semidefinite relaxation. In addtion, it could be proved that $\mathbf{H}(\lambda)$ has corank 1, thus $\mathrm{rank}(\mathbf{Y}) = 1$ and $\mathbf{y}$ is the unique optimum of (7).

Proof. The rank of $\mathbf{F}$ is equal to $\mathrm{rank}(\mathbf{A}) = 3 + N$ and the column number of $\mathbf{F}$ is $4 + N$, thus $\mathrm{corank}(F) = 4 + N - (3 + N) = 1$. Similarly, $\mathrm{corank}(\mathbf{G}_i) = 1, i = 1, ..., 2N$. Therefore, $\mathbf{H}(\lambda)$ has corank 1.

C. Tightness in a noisy case

In the Section B, we have derived the necessary conditions for tight relaxation and proved $\mathrm{rank}(\mathbf{Y}) = 1$ always exists. In this section, we discuss the necessary conditions for relaxation tightness with noisy measurements. Many previous works have proved that under mild noise perturbation, the strong duality of QCQP is preserved [20]. Similarly, we apply a regularity theorem for prior noise analysis [31] and derive a simulated noise bound in the follows.

Noise Perturbation. At the beginning, we define the parameters perturbed by noises. Since the ground receiver is known static, we assume that the velocity of the ground receiver is noise-free. Therefore, we only consider the noises from Doppler measurements and satellite positions/velocities. We use subscript θ to denote the perturbed function and matrix. These assumptions imply that the perturbed parameters only appear in the objective function $f_\theta(\mathbf{y})$ but not in the constraints $g_i(\mathbf{y}), i = 1, ..., N$.

Constraint Qualification. In noiseless cases, we assume that under KKT conditions *rank-tightness* is guaranteed and the Lagrange multipliers λ always exists. Nevertheless, in the noise cases, we need more regularity conditions to guarantee the existence of λ_θ. Here we follow the method in [30] to apply Abadie constraint qualification (ACQ) for an analytical noise bound. To guarantee the KKT conditions, we employ the Theorem 3.11 in [30], and modify it with general Wyle's inequality to get the noise regularity condition for our QCQP (7):

PROPOSITION 1 (Guaranteed noise bound)

$$\frac{1}{\sigma_N}\|\mathcal{G}\|\|\nabla f_\theta(\overline{\mathbf{y}})\| + \|\mathbf{F} - \mathbf{F}_\theta\| < \nu_{N+4}(\mathbf{F}_\theta) \qquad (14)$$

where $\overline{\mathbf{y}}$ presents the optimal variable in noiseless cases; σ_N is the N-th largest singular value of the gradient matrix of equation constraint, i.e. $\nabla g(\overline{\mathbf{y}})$; $\mathcal{G}$ is the sum of $\mathbf{G_i}, i = 1,...,N$; $\nabla f_\theta(\overline{\mathbf{y}})$ is the perturbed gradient of the objective function with the optimal variable $\overline{\mathbf{y}}$; $\mathbf{F}_\theta$ is the coefficient matrix with perturbed parameters; $\nu_{N+4}(\mathbf{F}_\theta)$ denotes the $(N+4)$-th smallest eigen value of $\mathbf{F}_\theta$. Interestingly, although the certification of optimality is performed after optimization, which is a posterior method, we can still quantify the possible noisy bound in simulation, which is a simulated prior method.

V. Experiments

The goal of this section is to (i) show that our certifiable method can outperform local searching methods in estimating the global optimum without initial estimates; (ii) test the performance of key modules, including GWA, SDP relaxation tightness, SDP optimality; (iii) show an application on LEO Doppler positioning using signal of opportunity (SOP). To achieve the goal, both simulation and real-world experiments are conducted with typical configurations to show the robustness and effectiveness of the proposed method. Note that since we use the Doppler measurements to estimate the receiver position in the Earth-Centered Earth-Fixed (ECEF) frame, positions and velocities may differ by several orders of magnitude. However, current off-the-shelf SDP solvers require the parameters to be close. To reduce this burden, we multiply the position and range variables (m) by 10^{-7}, and the velocity variable and Doppler measurements (m/s) by 10^{-3}. As a tradeoff, the solution of the proposed certifiably optimal method is not as precise as the local searching methods. Therefore, we also use the optimal but poor precision solution as initialization for local searching methods. All methods to be compared include:

1. **GN**: the Gauss-Newton (GN) method, by using linear approximation to estimate the NWLS problem iteratively [27];

2. **DL**: the Dog-Leg (DL) method, by using both Gauss-Newton steps and steepest steps within a trust region to solve the NWLS problem [32];

3. **SDP**: the proposed certifiably optimal method based on SDP, by solving the relaxed SDP and checking tight

3D positioning error with initial points ranged from different initial distance in the simulation test.

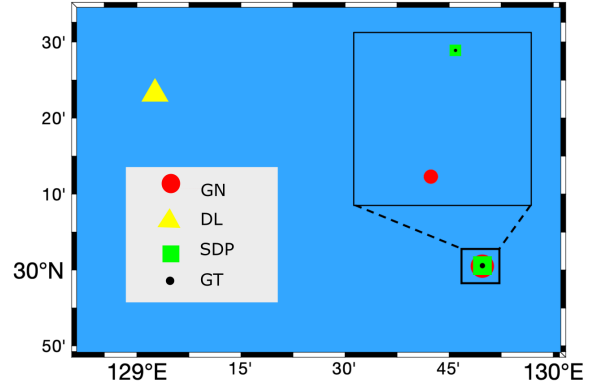| Init dist [km]	GN	DL	SDP	SDP-GN	SDP-DL
1	0.00	0.00	0.71	0.00	0.00
10	0.00	0.00	0.71	0.00	0.00
100	0.00	0.00	0.71	0.00	0.00
580	1839.60	91.65	0.71	0.00	0.00
1000	-	892.23	0.71	0.00	0.00

Fig. 3. Estimated position with the initial distance of 580 km, where 'GT' denotes ground-truth and other legends can be referred to Section A.

relaxation conditions to recover the global optimum of the NWLS problem [17].

4. **SDP-GN**: the SDP + GN method, using the solution from the method 3 (SDP) as initial estimation for the method 1 (GN) to solve the NWLS problem;

5. **SDP-DL**: the SDP + DL method, using the solution from the method 3 (SDP) as initial estimation for the method 2 (DL) to solve the NWLS problem.

For fair comparison, we implement all these methods in MATLAB R2024b, using the "sedumi" solver in CVX [17] to solve the SDP (11). Our experiment computer is a Macbook Pro 2017 with an Intel Core i5 CPU (2.3 GHz) and 8 GB LPDDR3 of RAM. To avoid confusion in numerical settings, we consider the SDP result as rank-tightness (i.e. globally optimal) when: (1) 'Solved' status from the CVX toolbox is obtained and (2) the ratio of the largest and second largest eigenvalue from variable $\mathbf{S}$ is greater than 10^5.

A. Simulation settings

We first conduct a simulation test to evaluate performance of the proposed certifiably correct method under ideal conditions. To simulate LEO Doppler measurements, we synthesize 49 LEO satellites uniformly distributed in a $1500 \times 1500\ km$ square on a spherical surface over the height of 800 km. The velocity of the satellites are simulated according to the Law of Gravity [33]. We

choose the projection of the satellites network center on the Earth surface as the ground receiver. The simulation model of Doppler measurements is (1) and intermediate frequency of the carrier wave is $1.626 \times 10^9 Hz$. With abundant measurements, we can ignore the effect of geometry distribution. To avoid occasionality, we repeat the Monte-Carlo simulation 40 times for each test to get the mean results. With the simulation data, we perform analysis in two main cases: noiseless and noisy cases. In the noiseless case, we focus on optimality analysis of the compared methods given different initial receiver positions. In the noisy case, we test the robustness of key modules under various kinds of mild parameter noises.

B. Discussion: Performance of positioning in noiseless cases

The result in the noiseless case is shown in Table I. According to the results, given exact initial distances, such as 1, 10 and 100 km, both GN and DL can estimate the position with 3D error of 0.04 m (0.00 km). As the initial distance from the ground truth increases to 580 km, the positioning error of GN increases to 1839.60 km and the error of DL comes to 91.65 km, not the same as the former case. When the initial distance comes to 1000 km, GN fails to output a feasible solution while the error of DL comes to 892.23 km. Although DL is less sensitive to the precision of initial estimates than GN, it still might provide wrong estimation. The changes of the results prove that: for local optimization methods, the initial variable value must be exact enough otherwise the optimization might converge to a local optima [16]. Compared to the local searching methods, the proposed SDP method is based on convex optimization, thus it does not need initial estimation. The reuslt show that SDP always converges to the same certified global minimum with a positioning error of 0.71 km. Compared with local searching methods, the proposed SDP method output certifiably optimal solutions but degrades in positioning precision. We speculate these reasons for the phenomenon: (1) numerical computing loss due to the magnitude difference between position and velocity in ECEF frame; (2) the relaxation is not tight enough and it still needs redundant constraints (similar to [31]); (3) accuracy limitation in CVX package [17]. To raise the accuracy of the certifiably optimal positioning, solution from SDP is also applied to GN and DL as their initial estimates. Although the result from local searching methods is heuristic, it can be proved that the combination of SDP and local searching methods is able to provide precise positioning results without prior initial estimation. Finally, an example of all positioning results with the initial distance of 580 km (initialization is only used for GN and DL) is illustrated in Fig. 3.

In conclusion, this noiseless simulation test show that the local estimation methods are sensitive to initializing estimation and might be trapped i local optima, even under noiseless conditions, while the convex estimation method SDP does not need initial guess. Together, current
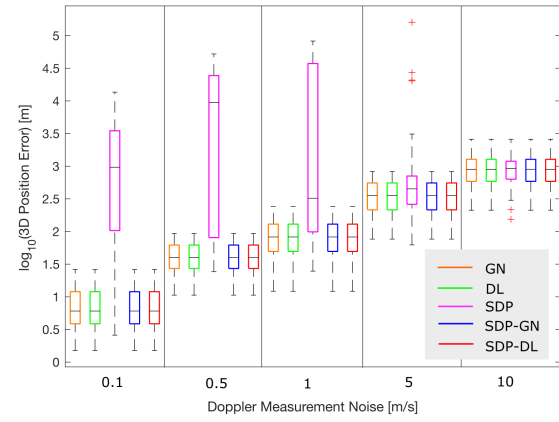

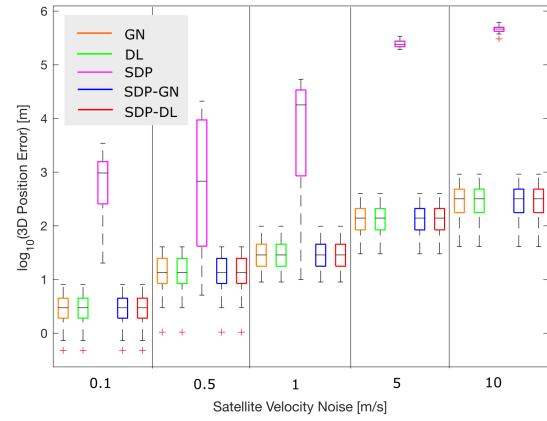Fig. 4. Satellite position error with the change of Doppler measurement noise

Fig. 5. Satellite position error with the change of satellite velocity noise

SDP solver CVX is affected by precision loss in LEO Doppler positioning problem, which could be enhanced by using SDP solution as the initialization for local searching methods.

C. Discussion: Performance of positioning in noisy cases

Here we analyze the performance of the proposed method with perturbed parameters in noisy cases. We aim to show that the optimality is guaranteed under mild noise disturbances. We provide additive zero-mean Gaussian noise to satellite position, velocity and Doppler measurements to simulate the real data in open-sky environments. (i) *Satellite position and velocity.* We first discuss the effect of the satellite position and velocity noise. Usually in SOP positioning, two-line-element (TLE) files and SGP4 model are used as ephemeris. The accuracy of TLE is about 1 km at the orbit determination epoch [6]. Here
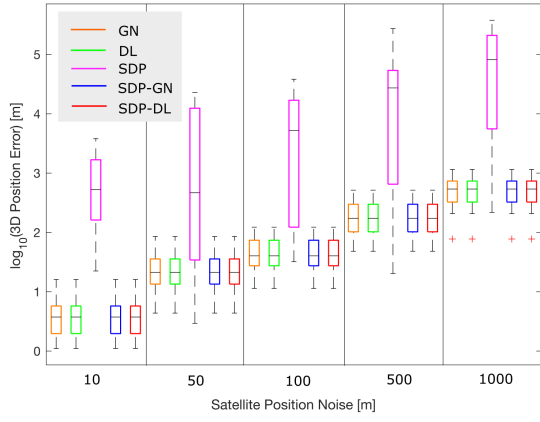
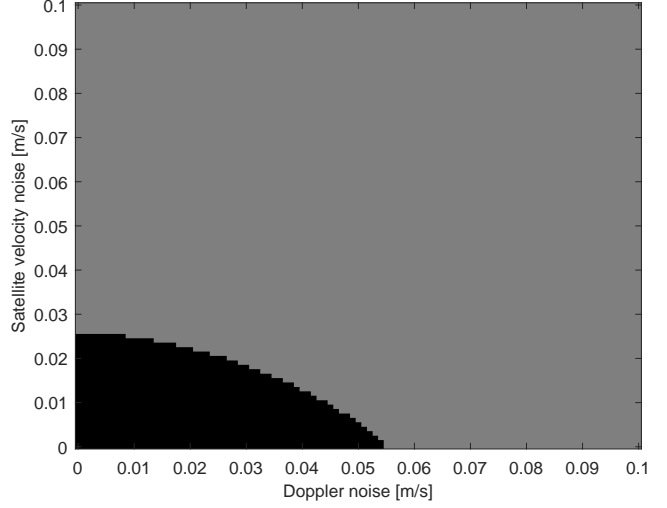Fig. 6.   3D positioning error with satellite position noises

Fig. 7.   Demonstration of explicit noise bound, including satellite velocity and Doppler measurement noises, where grey cells denote rank-tightness and black cells denote explicit bounded noise.

we simulate the position noise with a standard deviation (STD) up to 1 km and the velocity noise STD up to 50 m/s. (ii) *Doppler measurement.* Many works have evaluated the effect of all kinds of Doppler modelling noises, such as Earth rotating delay, atmospheric delay [16], and receiver clock shift rate [10]. Among these noises, the most significant one should be ionospheric delay, which could be up to 29 m/s in simulation [16]. Thus we simulate the Doppler noise up to 1000 m/s. The errors corresponding to Doppler shift, velocity and position noise disturbance are shown in Fig. 4, Fig. 5 and Fig. 6 separately. These results show that the positioning errors of two local searching methods are similar when exact initial estimation is given. Among these three kinds of noises, the satellite position noise contributes the most. We consider this is because the satellite position noise is absorbed in both the objective function and the constraint function in SDP (11). Thus noises in satellite positions could change both the feasible region and the relaxation tightness. Besides, we also recommend readers to [23] for the analysis on disturbed Cramér-Rao Lower Bound, CRLB. Luckily, although our proposed SDP is affected by the numerical accuracy limitation of MATLAB, it can still provide robust initialization for local searching methods. Under given mild noises, SDP-GN and SDP-DL reach the same error level as GN and DL using exact initialization from the ground truth.

D. Discussion: Noise bound for rank-tightness and global optimality

Together, since the optimality is certified after solving the SDP, we also evaluate sufficient noise bounds for satellite velocity and Doppler measurement parameters before solving the SDP according to Section C. The relationship between noise and rank-tightness is discussed in this section. According to (14), we evaluate the sufficient noise bound derived from ACQ and Wyle's inequality in Section C. Based on Theorem 3.11 from [30], we

TABLE II
Key parameters in the real experiment.

Dataset	LEO Doppler positioning
Constellation	Iridium (66 satellites in operation)
Orbit	Polar orbit ∼780 km altitude
Frequency	1626270833 Hz
Receiver Location	(22.3045966°, 114.180121°,61.384 m)
Visible Satellite	8
Duration	35 s
Measurements	436
Ephemeris	TLE+SGP4

simulate the estimated sufficient parameter noise bound for global optimality with perturbed parameters in the cost function of QCQP (7). The simulated result is illustrated in Fig. 7. Each cell corresponds to rank-tightness status, i.e., global optimality, of the SDP relaxation in our method. Among the cells, both the grey and black ones denote rank-tightness. Specially, the black cells present the our predicted noise bound. This figure shows that the ACQ and Wyle's inequality indeed give us a weak noise bound for rank tightness, around 2.5×10^{-2} m/s for satellite velocity noise and 5.5×10^{-2} m/s for Doppler measurement noise. This could be meaningful for users to evaluate the performance of our SDP-based method in their own applications. This sufficient noise bound for rank-tightness costs less computing time since we can perform it before time-cost SDP optimization process. The only limitation is that we have not derived the noise bound of position yet and current noise bounds are conservative. Although the predicted sufficient noise bound is more conservative than the actual one, this simulation is the first prior noise bound analysis and we can also derive a tight bound for all parameters in the future.
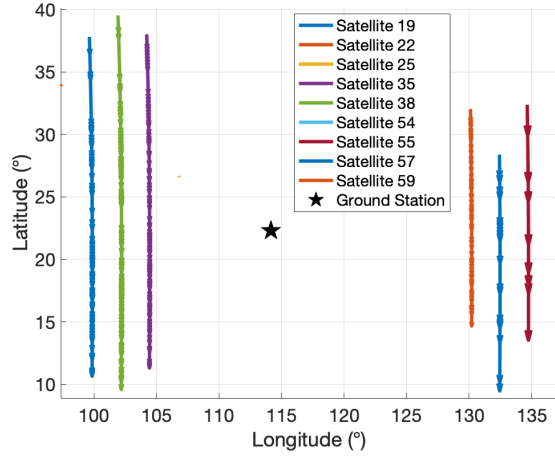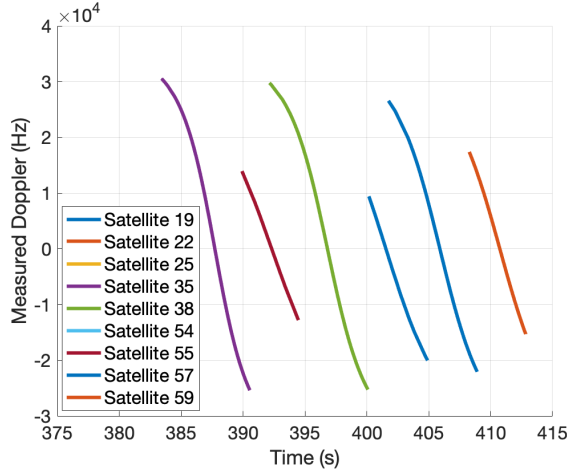
Fig. 8.   TLE+SGP4 ephemerides

Fig. 9.   Doppler shift measurements

E.   Real-world test

After discussion on effectiveness and limitation of the proposed method in simulation tests, we apply our method on a Iridium Doppler shift dataset collected by a software-defined ratio (SDR) system. We conduct the data collection at the campus of The Hong Kong Polytechnic University and the details of the dataset is shown in Table II. Since the geometric distribution of LEO satellites changes quickly, this dataset in about 35 seconds consists of 436 Doppler shift measurements from 8 satellites. The trajectory of the satellite is illustrated in Fig. 8, including positions and velocities. The Doppler shift measurements are illustrated in Fig. 9.

Then, similar to the simulation tests, we compare the performance of positioning using different initial positions. The results are shown in Table III. According to the results, we can find that the 3D positioning errors of GN and DL are 0.13 km when initial distance is 10 or 100 km. However, when the initial distance is equal or larger than 1000 km, these local searching methods

3D positioning errors of the compared methods using different initial distances in the real test.

Init dist [km]	GN	DL	SDP	SDP-GN	SDP-DL
10	0.13	0.13	0.14	0.13	0.13
100	0.13	0.13	0.14	0.13	0.13
500	0.13	0.13	0.14	0.13	0.13
1000	2342.50	2069.00	0.14	0.13	0.13
5000	-	8445.10	0.14	0.13	0.13

Fig. 10.   Local minima vs. Global minimum on Google Earth when the initial distance is 1000 km.

provide positioning far away from the ground truth. The 3D errors of GN and DL are 2342.50 km and 2069.00 km. Moreover, GN even fails to output a feasible solution while DL still output a position with error up to 8445.10 km. Compared with the local searching methods, the SDP method (ours) always estimates the globally optimal solution with its 3D error of 0.14 km. Together, after applying SDP solution to the local searching methods, both SDP-GN and SDP-DL achieve stable positioning while their error are the same as the best results in GN and DL, with 3D error of 0.13 km. The location results of all methods when the initial distance is 1000 km are illustrated on the Google Earth map. The results in the real experiment lead to similar phenomenons as the simulation tests. In summary, the proposed certifiably optimal method can output a globally optimal result without initialization. At the same time, after applying our SDP method as initialization, the enhanced local searching methods (SDP-GN and SDP-DL) also reach the global optimum, which is about horizontally 122 meters from the ground truth.

VI.   Conclusion

In this work, we develop a certifiably optimal estimation method to solve the LEO Doppler positioning problem. Our method does not require an initial guess, whereas other local estimation methods may fail due to inexact initialization. We also analysis the optimal-

ity guarantees for certifiably optimal estimation. The beneficial properties of our method are demonstrated via simulation and real-world tests. To the best of our knowledge, our method is the first certifiably optimal LEO Doppler positioning method. For the development of the community, we open-source our code and datasets. We believe that certifiably optimal navigation is a meaningful direction in the future.

The key technique in this work is convex optimization, which is popular in robotics and perception community. To employ it to the satellite navigation fields, there are opportunities and also challenges. For example, we only approach the static Doppler-based positioning problem. In the future, it is possible to estimate the position, velocity, clock drift at the same time by modeling navigation as a polynomial optimization problem (POP). We can possibly employ the moment sum-of-squares (SOS) method to solve it if we can find the conditions to reach relaxation tightness.

REFERENCES

[1] B. Eissfeller, T. Pany, D. Dötterböck, and R. Förstner
A comparative study of leo-pnt systems and concepts
In *Proceedings of the ION 2024 Pacific PNT Meeting*, Honolulu, Hawaii, Apr. 2024, pp. 758–782. [Online]. Available: https://doi.org/10.33012/2024.19646

[2] W. Wen, X. Bai, and L.-T. Hsu
3d vision aided gnss real-time kinematic positioning for autonomous systems in urban canyons
NAVIGATION: Journal of the Institute of Navigation, vol. 70, no. 3, p. 590, 2023. [Online]. Available: http://navi.ion.org/lookup/doi/10.33012/navi.590

[3] P. Wang, Y. Wang, E. Cetin, A. G. Dempster, and S. Wu
Gnss jamming mitigation using adaptive-partitioned subspace projection technique
IEEE Transactions on Aerospace and Electronic Systems, vol. 55, no. 1, pp. 343–355, 2018.

[4] L. Bai, C. Sun, A. G. Dempster, H. Zhao, and W. Feng
Gnss spoofing detection and mitigation with a single 5g base station aiding
IEEE Transactions on Aerospace and Electronic Systems, vol. 60, no. 4, pp. 4601–4620, 2024.

[5] Z. M. Kassas, J. Khalife, A. A. Abdallah, and C. Lee
I am not afraid of the gps jammer: Resilient navigation via signals of opportunity in gps-denied environments
IEEE Aerospace and Electronic Systems Magazine, vol. 37, no. 7, pp. 4–19, 2022.

[6] J. Khalife, M. Neinavaie, and Z. M. Kassas
The first carrier phase tracking and positioning results with starlink leo satellite signals
IEEE Transactions on Aerospace and Electronic Systems, vol. 58, no. 2, pp. 1487–1491, 2021.

[7] N. S. Miller *et al.*
Snap: A xona space systems and gps software-defined receiver
In *2023 IEEE/ION Position, Location and Navigation Symposium (PLANS)*. IEEE, 2023, pp. 897–904.

[8] R. Deng, H. Qin, H. Li, D. Wang, and H. Lv
Noncooperative leo satellite orbit determination based on single pass doppler measurements
IEEE Transactions on Aerospace and Electronic Systems, vol. 59, no. 2, pp. 1096–1106, 2022.

[9] D. Wang, H. Qin, and Z. Huang
Doppler positioning of leo satellites based on orbit error compensation and weighting

[10] F. Guo, Y. Yang, F. Ma, Y. Zhu, H. Liu, and X. Zhang
Instantaneous velocity determination and positioning using doppler shift from a leo constellation
Satellite Navigation, vol. 4, no. 1, p. 9, 2023.

[11] T. A. Stansell
Transit, the navy navigation satellite system
NAVIGATION: Journal of the Institute of Navigation, vol. 18, no. 1, pp. 93–109, 1971.

[12] J. C. McDowell
The low earth orbit satellite population and impacts of the spacex starlink constellation
The Astrophysical Journal Letters, vol. 892, no. 2, p. L36, 2020.

[13] C. Yang *et al.*
Doppler positioning of dynamic targets with unknown leo satellite signals
Electronics, vol. 12, no. 11, p. 2392, 2023.

[14] T. E. Humphreys, P. A. Iannucci, Z. M. Komodromos, and A. M. Graff
Signal structure of the starlink ku-band downlink
IEEE Transactions on Aerospace and Electronic Systems, vol. 59, no. 5, pp. 6016–6030, 2023.

[15] M. A. Hasan, M. H. Kabir, M. S. Islam, S. Han, and W. Shin
A double-difference doppler shift-based positioning framework with ephemeris error correction of leo satellites
IEEE Systems Journal, 2024.

[16] C. Shi, Y. Zhang, and Z. Li
Revisiting doppler positioning performance with leo satellites
GPS Solutions, vol. 27, no. 3, p. 126, 2023.

[17] S. P. Boyd and L. Vandenberghe
Convex Optimization. Cambridge University Press, 2004.

[18] H. Yang, J. Shi, and L. Carlone
Teaser: Fast and certifiable point cloud registration
IEEE Transactions on Robotics, vol. 37, no. 2, pp. 314–333, 2020.

[19] M. Giamou, Z. Ma, V. Peretroukhin, and J. Kelly
Certifiably globally optimal extrinsic calibration from per-sensor egomotion
IEEE Robotics and Automation Letters, vol. 4, no. 2, pp. 367–374, 2019.

[20] D. M. Rosen, L. Carlone, A. S. Bandeira, and J. J. Leonard
Se-sync: A certifiably correct algorithm for synchronization over the special euclidean group
The International Journal of Robotics Research, vol. 38, no. 2-3, pp. 95–125, 2019.

[21] H. Liu, X. Li, and A. M.-C. So
Resync: Riemannian subgradient-based robust rotation synchronization
In *Advances in Neural Information Processing Systems*, vol. 36, 2023, pp. 5236–5261.

[22] P. Kaveti, M. Giamou, H. Singh, and D. M. Rosen
Oasis: Optimal arrangements for sensing in slam
In *2024 IEEE International Conference on Robotics and Automation (ICRA)*. IEEE, 2024, pp. 13 818–13 824.

[23] L. Deng, P. Wei, Z. Zhang, and H. Zhang
Doppler frequency shift based source localization in presence of sensor location errors
IEEE Access, vol. 6, pp. 59 752–59 760, 2018.

[24] Y. Yan, G. Yang, H. Wang, and X. Shen
Robust multiple sensor localization via semidefinite relaxation in wireless sensor networks with anchor position uncertainty
Measurement, vol. 196, p. 111193, 2022.

[25] B. Song, W. Wen, and L.-T. Hsu
Certifiably optimal satellite orbit determination based on doppler measurements for low-earth-orbit satellites
In *2025 IEEE/ION Position, Location and Navigation Symposium (PLANS)*, 2025, pp. 410–416.

[26] M. S. Bazaraa, H. D. Sherali, and C. M. Shetty

Nonlinear Programming: Theory and Algorithms. John Wiley & Sons, 2006.

[27] S. Gratton, A. S. Lawless, and N. K. Nichols
Approximate gauss–newton methods for nonlinear least squares problems
SIAM Journal on Optimization, vol. 18, no. 1, pp. 106–132, 2007.

[28] Y. T. Chan and K. C. Ho
A simple and efficient estimator for hyperbolic location
IEEE Transactions on Signal Processing, vol. 42, no. 8, pp. 1905–1915, 1994.

[29] H. Yang and L. Carlone
A polynomial-time solution for robust registration with extreme outlier rates
arXiv preprint arXiv:1903.08588, 2019. [Online]. Available: https://arxiv.org/abs/1903.08588

[30] D. Cifuentes, S. Agarwal, P. A. Parrilo, and R. R. Thomas
On the local stability of semidefinite relaxations
Mathematical Programming, vol. 193, no. 2, pp. 629–663, 2022.

[31] F. Dümbgen, C. Holmes, B. Agro, and T. Barfoot
Toward globally optimal state estimation using automatically tightened semidefinite relaxations
IEEE Transactions on Robotics, vol. 40, pp. 4338–4358, 2024.

[32] S. Wright and J. Nocedal
Numerical optimization
Springer Science, vol. 35, no. 67-68, p. 7, 1999.

[33] Y. Zhuang and L. Wang
Analysis of the gravity models impact on leo satellite orbit prediction
The International Archives of the Photogrammetry, Remote Sensing and Spatial Information Sciences, vol. 46, pp. 307–313, 2022.